Workshop on Material Appearance Modeling (2020)
H. Rushmeier and R. Klein (Editors)

A Genetic Algorithm Based Heterogeneous Subsurface Scattering Representation

Murat Kurt[1†]

[1]International Computer Institute, Ege University

Abstract

In this paper, we present a novel heterogeneous subsurface scattering (sss) representation, which is based on a combination of Singular Value Decomposition (SVD) and genetic optimization techniques. To find the best transformation that is applied to measured subsurface scattering data, we use a genetic optimization framework, which tries various transformations to the measured heterogeneous subsurface scattering data to find the fittest one. After we apply the best transformation, we compactly represent measured subsurface scattering data by separately applying the SVD per-color channel of the transformed profiles. In order to get a compact and accurate representation, we apply the SVD on the model errors, iteratively. We validate our approach on a range of optically thick, real-world translucent materials. It's shown that our genetic algorithm based heterogeneous subsurface scattering representation achieves greater visual accuracy than alternative techniques for the same level of compression.

Categories and Subject Descriptors (according to ACM CCS): I.3.7 [Computer Graphics]: Three-Dimensional Graphics and Realism—Color, shading, shadowing, and texture

1. Introduction

In the field of computer graphics, photo-realistic representation of optically thick, translucent materials requires modeling of the Bidirectional Surface Scattering Distribution Function (BSSRDF), which is a generalization of the Bidirectional Reflectance Distribution Function (BRDF) introduced by Nicodemus et al. [NRH*77]. Wax, marble, human skin, and leaves are good examples of translucent materials, and they exhibit complex light scattering behaviors due to subsurface scattering. Optically thick, translucent materials can be decomposed into two classes, namely homogeneous and heterogeneous. While optical properties of homogeneous translucent materials are constant, heterogeneous translucent materials exhibit spatially varying optical behaviors [Kur20]. Therefore, measuring and modeling of heterogeneous translucent materials are much more complicated than homogeneous translucent materials, and requires much better understanding of light and material interactions beneath the surface.

The diffusion equation is a well-known approximation technique, that is used to represent homogeneous translucent materials [FJB04]. The most of the homogeneous subsurface scattering models used in the computer graphics community are derived based on this approximation [JMLH01, JB02, FHK14, JZJ*15]. As the optical properties of heterogeneous translucent materials exhibit spatially varying distributions, measuring the optical properties of heterogeneous translucent materials results in the large data sizes [NK18, YTYM20, FJM*20]. Therefore, a number of data-driven subsurface scattering representations [PvBM*06, STPP09, KOP13, YTYM20, Kur20] have been proposed to represent measured heterogeneous subsurface scattering data, compactly and accurately. But, it's still an investigation issue to represent measured heterogeneous subsurface scattering data compactly and physically accurately.

To represent measured heterogeneous subsurface scattering data compactly and accurately, we propose to use a combination of Genetic Algorithm (GA) [Mit96] and Singular Value Decomposition (SVD) [PSR13] techniques. We try various transformations to find the best transformation by using our genetic optimization framework. Our GA helps us to find the fittest transformation that is applied to the profiles of measured subsurface scattering data. Then, we compress these transformed profiles by using a rank-1 approximation of the SVD technique [PSR13]. We repeatedly apply the rank-1 approximation on the model errors to achieve a compact and accurate representation (see Algorithm 1). Our empirical results show that our GA based subsurface scattering representation provides satisfactory approximations for the measured heterogeneous subsurface scattering data.

2. Our Subsurface Scattering Representation

The general behavior of translucent materials is described by the BSSRDF [NRH*77] $S(x_i, \vec{\omega}_i; x_o, \vec{\omega}_o)$, which is used to compute an outgoing radiance $L_o(x_o, \vec{\omega}_o)$ at a location x_o in an outgoing direction $\vec{\omega}_o$. This computation can be separated into two com-

† e-mail: murat.kurt@ege.edu.tr

DOI: 10.2312/mam.20201140

Table 1: *Properties of the genetic optimization for heterogeneous artificial stone. The table also summarizes some statistics of transformations applied by our genetic algorithm with $K = 1$. When we don't apply any transformations, the rank-1 approximation of artificial stone gives a RMSE of* 0.10091.

Transformation ID	Transformation expression	Chromosome	Population size	Fittest value (RMSE)
1	$R''_d(x_i,d) = \ln\left(1+\frac{R'_d(x_i,d)}{\alpha_s}\right)$	$\alpha_s(R,G,B)$	30	0.09694
2	$R''_d(x_i,d) = \ln\left(\alpha_d+\frac{R'_d(x_i,d)}{\alpha_s}\right)$	$\alpha_d(intensity), \alpha_s(intensity)$	20	0.09699
3	$R''_d(x_i,d) = \begin{cases} R'_d(x_i,d)/max(R'_d(x_i,d)) & if\, range = 0 \\ \ln\left(1+\frac{R'_d(x_i,d)}{\alpha_s max(R'_d(x_i,d))}\right) & otherwise \end{cases}$	$\alpha_s(R,G,B),\ d \pm range(R,G,B)$	60	0.09340

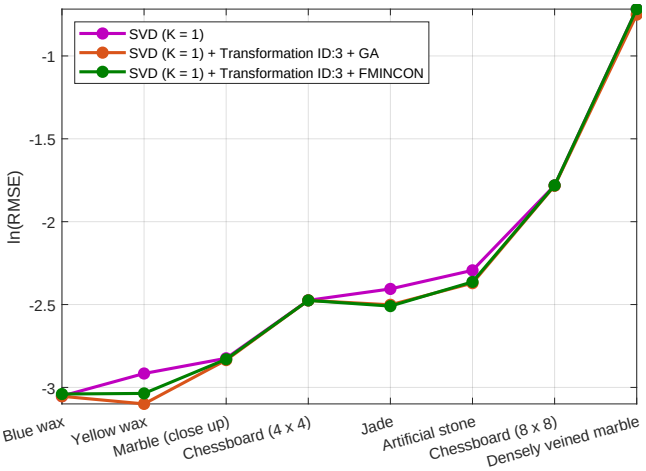

Figure 1: *A comparison of the SVD based subsurface scattering model with and without applying various optimization techniques (see Table 1). The model parameter K was selected as 1. The error values were sorted in the logarithmic RMSEs of the SVD technique (purple) for visualization purposes.*

ponents; a local component $L_l(x_o, \vec{\omega}_o)$ and a global component $L_g(x_o, \vec{\omega}_o)$. The global component accounts for the light scattering within the material volume, and it can be represented using the diffuse BSSRDF $S_d(x_i, \vec{\omega}_i; x_o, \vec{\omega}_o)$, which can be further decomposed approximately [JMLH01, PvBM*06, STPP09]:

$$S_d(x_i, \vec{\omega}_i; x_o, \vec{\omega}_o) = \frac{1}{\pi} F_i(x_i, \vec{\omega}_i) R_d(x_i, x_o) F_o(x_o, \vec{\omega}_o). \quad (1)$$

In this work, we focus on representing $R_d(x_i, x_o)$, which is a four dimensional (4D) spatial subsurface scattering component by neglecting other components (i.e., the local component $L_l(x_o, \vec{\omega}_o)$ and the directional dependent components $F_o(x_o, \vec{\omega}_o)$ and $F_i(x_i, \vec{\omega}_i)$) assuming light incoming from the surface normal.

To represent $R_d(x_i, x_o)$ compactly, we linearize the measured 4D input data to a two dimensional (2D) form, i.e., matrix. After that, we reshape the subsurface scattering matrix $R_d(x_i, x_o)$ by changing the variables $d = x_o - x_i$ to get $R'_d(x_i, d)$, which can be further decomposed instead of $R_d(x_i, x_o)$ [PvBM*06, KOP13, Kur20]. To find the best transformation for measured $R'_d(x_i, d)$ data, we try various transformations using our GA to measured data sets from Peers et al. [PvBM*06] and Song et al. [STPP09]. The GA is a machine learning technique for solving both constrained and unconstrained optimization problems by imitating biological evolution processes including natural selection [Mit96]. We apply GA to find new transformations for real-world subsurface scattering. The key idea behind a GA is that it repeatedly updates a population of individual solutions, culling undesirable ones and allowing the fittest ones to survive. A single such individual solution is referred to as a chromosome, and each element of the chromosome is referred to as a gene. At each step the algorithm selects solutions at random, from the current population. These are treated as parents and the algorithm uses these to produce children for the next generation. Over successive generations, the population evolves toward an optimal solution based on a fitness function.

Algorithm 1 presents our genetic objective function, used in our genetic optimization framework. Algorithm 1 is used as an objective function in GA [Mit96] which is readily available in MATLAB library. In Algorithm 1, the *sum* function returns the sum of the elements if the input is a vector. If the input is a matrix, it returns a row vector containing the sum of each column. The *transOpt()* function applies a transformation operation to the input subsurface scattering data based on transformation ID (see Table 1), and the chromosome. The biological evolution of the chromosomes uses the GA implementation in MATLAB with selection, crossover and mutation operations. *invTransOpt()* applies an inverse transformation operation to the input data based on the transformation ID (see Table 1), and the chromosome. To factorize subsurface scattering data, Algorithm 1 uses SVDS [PSR13], also available in MATLAB. In Algorithm 1, SVDS applies a rank-1 factorization to the transformed subsurface scattering data. In Algorithm 1, we also use *pow* and *size* functions available in MATLAB library.

To get meaningful results, we apply boundary constraints to the values (i.e., genes) of the chromosomes thorough the GA, which allows adding both upper and lower bounds to the genes of the chromosome. We investigate various transformation and chromosome combinations (see Table 1) thorough Algorithm 1 together with the GA. Algorithm 2 reconstructs a subsurface scattering matrix using two vectors $(f(x_i), v(d))$ and a scalar value (s). Algorithm 2 is employed by Algorithm 1. In our investigation, transformation ID:3 is the fittest transformation, which can be seen in Table 1. We also applied both GA and FMINCON optimization techniques to find the fittest transformation in Figure 1. These optimization techniques are readily available in MATLAB library. On average, transformation ID:3 with GA and FMINCON decrease the RMSE by 3.835%, and 1.973%, respectively. Therefore, we select and use transformation ID:3 with our GA framework.

Our final subsurface scattering model will be the sum of the estimation of model errors and the first factorization of $R''_d(x_i,d)$, which can be formalized as:

$$R''_d(x_i,d) \approx \sum_{j=1}^{K} f_j(x_i)h_j(d), \tag{2}$$

K is the total number of terms, $f_j(x_i)$ and $h_j(d) = s_j v_j(d)$ are the univariate functions, which result in a very compact subsurface scattering representation.

Algorithm 1: geneticObjective(R'_d, K, ID, *chromosome*)

/*R'_{dr}, R'_{dg} and R'_{db} are color components of R'_d*/
let $R''_{dr} = transOpt(R'_{dr}, ID, chromosome)$
let $R''_{dg} = transOpt(R'_{dg}, ID, chromosome)$
let $R''_{db} = transOpt(R'_{db}, ID, chromosome)$
let $transSSS_r = transSSS_g = transSSS_b = 0$
let $estR'_{dr} = estR'_{dg} = estR'_{db} = 0$
let $sum_r = sum_g = sum_b = fitness = 0$
for $j = 1$ to K
  $[f_{rj}, s_{rj}, v_{rj}] = svds(R''_{dr}, 1)$
  $[f_{gj}, s_{gj}, v_{gj}] = svds(R''_{dg}, 1)$
  $[f_{bj}, s_{bj}, v_{bj}] = svds(R''_{db}, 1)$
  $R''_{dr} = R''_{dr} - genEvaluateSSS(f_{rj}, s_{rj}, v_{rj})$
  $R''_{dg} = R''_{dg} - genEvaluateSSS(f_{gj}, s_{gj}, v_{gj})$
  $R''_{db} = R''_{db} - genEvaluateSSS(f_{bj}, s_{bj}, v_{bj})$
end for
for $j = 1$ to K
  $transSSS_r = transSSS_r + genEvaluateSSS(f_{rj}, s_{rj}, v_{rj})$
  $transSSS_g = transSSS_g + genEvaluateSSS(f_{gj}, s_{gj}, v_{gj})$
  $transSSS_b = transSSS_b + genEvaluateSSS(f_{bj}, s_{bj}, v_{bj})$
end for
$estR'_{dr} = invTransOpt(transSSS_r, ID, chromosome)$
$estR'_{dg} = invTransOpt(transSSS_g, ID, chromosome)$
$estR'_{db} = invTransOpt(transSSS_b, ID, chromosome)$
$sum_r = sum(sum(pow(R'_{dr} - estR'_{dr}, 2)))$
$sum_g = sum(sum(pow(R'_{dg} - estR'_{dg}, 2)))$
$sum_b = sum(sum(pow(R'_{db} - estR'_{db}, 2)))$
$fitness = sqrt(1/(3 * size(R'_d, 1) * size(R'_d, 2)) * sum(sum_r + sum_g + sum_b))$
return $fitness$

Algorithm 2: genEvaluateSSS(f, s, v)

let $genSSS = 0$
for $i = 1$ to $size(f, 1)$
 for $j = 1$ to $size(v, 1)$
  $genSSS(i, j) = f(i) * s * v(j)$
 end for
end for
return $genSSS$

3. Results

In this work, we validate our model on 8 different real-world translucent materials. Table 2 gives an overview of the modeled heterogeneous translucent materials and lists a number of statistics for our model, based on typical values for K. We compare measured and modeled subsurface responses of selected surface points in Figure 2 (upper row). We also compare measured and modeled subsurface models in Figure 2 (bottom row). The SubEdit [STPP09] representation may show radially symmetric behavior at some materials (see blue wax in Figure 2), due to the parametrization used, which may be insufficient for representing heterogeneous materials accurately. The comparisons outlined show that our model represents heterogeneous translucent materials more accurately for comparable data storage requirements.

In this work, we present a GA based heterogeneous subsurface scattering model. In the future, we plan to investigate real-time rendering algorithms to implement our representation in screen-space.

Acknowledgements

The author would like to thank Pieter Peers et al. [PvBM*06] and Ying Song et al. [STPP09] for sharing their measured subsurface scattering data sets. This work was supported by the Scientific and Technical Research Council of Turkey (Project No: 119E092).

References

[FHK14] FRISVAD J. R., HACHISUKA T., KJELDSEN T. K.: Directional dipole model for subsurface scattering. *ACM Trans. Graph. 34*, 1 (Dec. 2014), 5:1–5:12. 1

[FJB04] FLEMING R. W., JENSEN H. W., BÜLTHOFF H. H.: Perceiving translucent materials. In *Proceedings of the 1st Symposium on Applied Perception in Graphics and Visualization* (2004), APGV '04, pp. 127–134. 1

[FJM*20] FRISVAD J. R., JENSEN S. A., MADSEN J. S., CORREIA A., YANG L., GREGERSEN S. K. S., MEURET Y., HANSEN P.-E.: Survey of models for acquiring the optical properties of translucent materials. *Computer Graphics Forum 39*, 2 (2020), 729–755. doi:10.1111/cgf.14023. 1

[JB02] JENSEN H. W., BUHLER J.: A rapid hierarchical rendering technique for translucent materials. *ACM TOG 21*, 3 (July 2002), 576–581. (Proc. SIGGRAPH '02). 1

[JMLH01] JENSEN H. W., MARSCHNER S. R., LEVOY M., HANRAHAN P.: A practical model for subsurface light transport. In *Proc. SIGGRAPH '01* (2001), pp. 511–518. 1, 2

[JZJ*15] JIMENEZ J., ZSOLNAI K., JARABO A., FREUDE C., AUZINGER T., WU X.-C., DER PAHLEN J., WIMMER M., GUTIERREZ D.: Separable subsurface scattering. *Comput. Graph. Forum 34*, 6 (Sept. 2015), 188–197. 1

[KOP13] KURT M., ÖZTÜRK A., PEERS P.: A compact tucker-based factorization model for heterogeneous subsurface scattering. In *Proceedings of the 11th Theory and Practice of Computer Graphics* (2013), TPCG '13, pp. 85–92. 1, 2

[Kur20] KURT M.: GenSSS: a genetic algorithm for measured subsurface scattering representation. *The Visual Computer* (2020). (Online Published). doi:10.1007/s00371-020-01800-0. 1, 2

[Mit96] MITCHELL M.: *An Introduction to Genetic Algorithms*. MIT Press, Cambridge, MA, USA, 1996. 1, 2

[NK18] NAKAMOTO K., KOIKE T.: Which BSSRDF model is better for heterogeneous materials? In *Proceedings of the ACM SIGGRAPH 2018, Posters* (2018), SIGGRAPH '18, pp. 44:1–44:2. 1

[NRH*77] NICODEMUS F. E., RICHMOND J. C., HSIA J. J., GINSBERG I. W., LIMPERIS T.: *Geometrical Considerations and Nomenclature for Reflectance*. Monograph, National Bureau of Standards (US), Oct. 1977. 1

Table 2: *Properties of the factored heterogeneous subsurface scattering materials. The table also summarizes some statistics of our GA based subsurface scattering model with typically selected values for K.*

Sample material	Resolution (pixel)	Kernel size (pixel)	Original size	K	Factored size	CR	RMSE
Chessboard (4×4)	277×277	39×39	2.61 GB	5	8.96 MB	1/298	0.0229
Chessboard (8×8)	222×222	39×39	1.68 GB	5	5.82 MB	1/296	0.0421
Marble (close up)	128×128	39×39	570 MB	5	2.05 MB	1/278	0.0268
Densely veined marble	213×211	39×39	1.53 GB	5	5.32 MB	1/295	0.0568
Artificial stone	108×108	35×35	327 MB	5	1.48 MB	1/222	0.0340
Blue wax	88×232	35×35	572 MB	5	2.48 MB	1/231	0.0192
Jade	260×260	35×35	1.85 GB	5	7.88 MB	1/240	0.0398
Yellow wax	110×110	39×39	421 MB	5	1.56 MB	1/270	0.0225

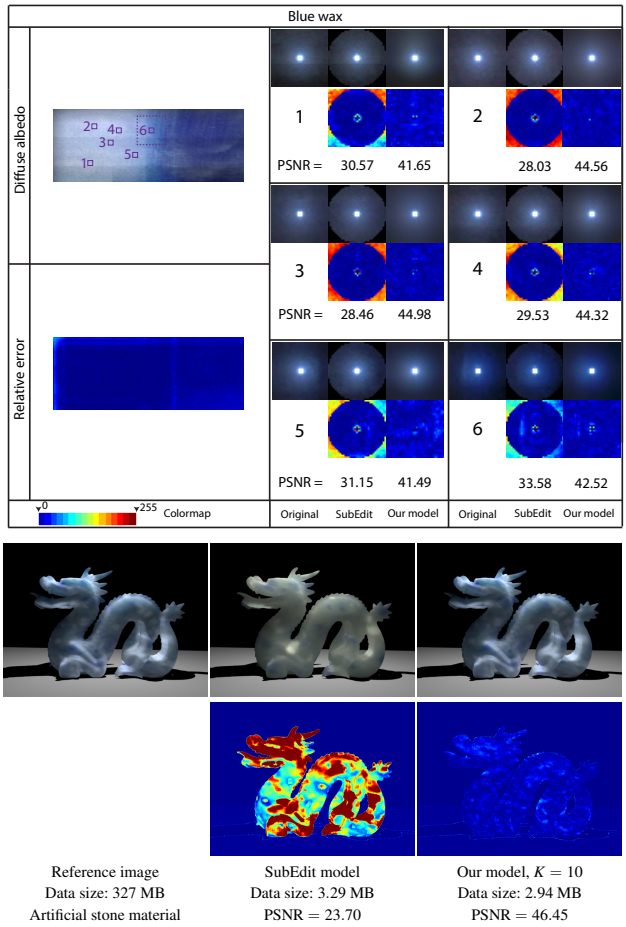

Reference image
Data size: 327 MB
Artificial stone material

SubEdit model
Data size: 3.29 MB
PSNR = 23.70

Our model, $K = 10$
Data size: 2.94 MB
PSNR = 46.45

Figure 2: *A response comparison (upper row) and a visual comparison (bottom row) between the SubEdit model [STPP09] and our model at comparable data sizes. We computed false-color difference images between measured data and corresponding approximations of models. Note that for better comparison, false-color differences were scaled by a factor of ten.*

[PSR13] PAJAROLA R., SUTER S. K., RUITERS R.: Tensor Approximation in Visualization and Computer Graphics. In *EG 2013 - Tutorials* (Girona, Spain, 2013), Eurographics Association, pp. t6–. 1, 2

[PvBM*06] PEERS P., VOM BERGE K., MATUSIK W., RAMAMOORTHI R., LAWRENCE J., RUSINKIEWICZ S., DUTRÉ P.: A compact factored representation of heterogeneous subsurface scattering. *ACM TOG 25*, 3 (July 2006), 746–753. (Proc. SIGGRAPH '06). 1, 2, 3

[STPP09] SONG Y., TONG X., PELLACINI F., PEERS P.: SubEdit: a representation for editing measured heterogeneous subsurface scattering. *ACM TOG 28*, 3 (July 2009), 31:1–31:10. (Proc. SIGGRAPH '09). 1, 2, 3, 4

[YTYM20] YATAGAWA T., TODO H., YAMAGUCHI Y., MORISHIMA S.: Data compression for measured heterogeneous subsurface scattering via scattering profile blending. *The Visual Computer 36*, 3 (2020), 541–558. doi:10.1007/s00371-018-01626-x. 1